Available online at www.sciencedirect.com

SciVerse ScienceDirect

Ceramics International 39 (2013) 1923–1929

CERAMICS INTERNATIONAL

www.elsevier.com/locate/ceramint

Preparation and characterization of foam ceramics from red mud and fly ash using sodium silicate as foaming agent

Xingjun Chen, Anxian Lu*, Gao Qu

School of Materials Science and Engineering, Central South University, Changsha 410083, PR China

Received 25 June 2012; received in revised form 24 July 2012; accepted 14 August 2012
Available online 21 August 2012

Abstract

Fly ash from the thermal power plant and red mud from aluminium industry were regarded as hazardous industry waste all over the world. In order to effectively utilize these industrial wastes, a new foam ceramics was synthesized successfully by conventional ceramic sintering process using fly ash and red mud as the main raw material, with a small amount of sodium borate as fluxing agent and sodium silicate as foaming agent. An objective of this research was to investigate the influences of the amounts of red mud/fly ash and sodium borate as well as of the sintering temperature on the porosity, mechanical strength, bulk density, water absorption, microstructure and crystalline phase. The results showed that homogeneous microstructures of large pores could be obtained by adding about 40–50 wt% red mud, 26.25–40 wt% fly ash, 15–20 wt% sodium borate, 5 wt% sodium silicate, and using low sintering temperature (900 °C, 2 h), leading to foams presenting porosity, compressive strength, flexural strength, bulk density, and water absorption values of about 64.14–74.15%, 4.04–10.63 MPa, 2.31–8.52 MPa, 0.51–0.64 g/cm^3, and 2.31–6.02%, respectively. Good correlations among mechanical strength, water absorption and microstructure (pore size and distribution) were observed.

Keywords: Red mud; Fly ash; Foam ceramics; Sodium silicate

1. Introduction

The huge volumes of industrial waste produced today represent one of the world's greatest environmental problems and recycling has emerged as a very important environmental issue nowadays due to the diminishing nature resources and the increasing amount of solid wastes. Red mud, as one of the major solid wastes, is produced in the process of alumina extraction from bauxite [1]. Due to its caustic nature, it poses a major environmental problem [2]. For every ton of alumina produced, approximately 1–1.5 tons of red mud is generated in the process [3]. In China currently only a small percentage of this waste is utilized, primarily in the cementitious products (concrete and cement) [4], the remainder being directly discharged into ponds or landfills, which is regarded as unsightly, environmentally undesirable and a non-productive use of land resources, as well as posing an on-going financial burden through their long-term maintenance. Therefore, utilization of red mud will produce significant benefits in terms of environment and economics by reducing landfill volume, contamination of soil and ground water, and release of land for alternative uses.

Fly ash is another waste residue produced as a by-product of coal combustion in power stations [5]. This industrial waste is regarded as hazardous material all over the world, which presents serious problems related to land disposal and environmental pollution [6]. However, in China, there are more and more thermal power plants being built today to satisfy the increasing demand for energy resources. And millions of tons of coal fly ash are produced each year. Therefore, the development of new applications for fly ash is necessary in order to reduce reliance on landfill and could be helpful not only in decreasing environmental pollution, but also in producing high value added products. And on the other hand, fly ash containing a large amount of CaO, SiO_2, and Al_2O_3, which are main glass network formers, can be a good raw material for the $CaO–Al_2O_3–SiO_2$ system of ceramic and glass-ceramic production [7].

*Corresponding author. Tel.: +86 731 88830351; fax: +86 731 88877057.
E-mail address: axlu@csu.edu.cn (A. Lu).

0272-8842/$ - see front matter © 2012 Elsevier Ltd and Techna Group S.r.l. All rights reserved.
http://dx.doi.org/10.1016/j.ceramint.2012.08.042

There are several researches on red mud and fly ash reuse; for example, Li et al. [8] evaluated the use of red mud and fly ash to remove toxic materials from waste water; Karasu et al. [9] investigated the effects of red mud based pigments on wall and floor tile glazes; Amritphale et al. [10] proposed a novel method for making radiation shielding materials utilizing red mud and other additives. Unfortunately, red mud reuse techniques consume relatively small amounts of waste, compared to a huge quantity of red mud discharged from the alumina production every year. Thus, in order to realize bulk use in red mud and fly ash, recently, the exploration has been focused on the construction and building industry [11,12], especial in light weight construction products. For example, Yang et al. [13] found that the addition of up to 40 wt% of red mud waste was possible in the production of the ceramics tiles; Sglavo et al. [14] has added 50 wt% red mud in clay-based ceramics; Yang et al. [15] successful synthesized glass-ceramics with the total addition of up to 85 wt% of red mud and fly ash. There are obvious environmental benefits to be gained from the recycling of wastes in producing ceramic tiles, ceramics and glass-ceramics. Unfortunately, some aspects limit their applications as well as their commercial success, such as impurities (Fe_2O_3, MnO) in the wastes which often color the final products [16], and the complex densification mechanism which limits the amount of waste that can be used when preparing dense products. Development of foam ceramics from red mud and fly ash might solve the problem. The porosity of foam ceramics makes it possess the properties of sound and thermal insulation [17] and it could be used as light weight construction materials. But little research has been conducted to focus on preparing the foam ceramics.

In our previous work, the waste-based foam glasses containing fly ash of 70 wt% have been successfully prepared by another group of ours [18,19]. In this study, authors firstly prepared foam ceramics using red mud and fly ash as raw materials simultaneously, and with sodium borate and sodium silicate as additives. The effects of different ratio of red mud and fly ash on sample properties were studied in detail, mainly including phase compositions, microstructure, porosity and mechanical properties. And also, the effects of fluxing agent sodium borate as well as different sintering temperatures on the main properties of foam ceramics were studied. Foam ceramics may have a good application in the market of light weight construction materials because of its lower energy consumption and costs in the current process, and may play an important role to eliminate the storage of red mud in China.

2. Experimental

2.1. Raw materials

Red mud and fly ash used in the present experiment were supplied by Henan Aluminum Co. Ltd. and Changsha Power Plant, respectively. The chemical compositions of red mud and fly ash were determined by X-ray fluorescence analysis and the results are shown in Table 1. XRD analysis was used to investigate the crystalline phase of the raw materials, and the XRD patterns are shown in Figs. 1 and 2. As shown in Fig. 1, the major crystalline phases in fly ash are Quartz SiO_2 (PDF no. 8590798) and Mullite $Al_6Si_2O_{13}$ (PDF no. 15-0776). As shown in Fig. 2, the major mineral phases in red mud are identified as Katoite $Ca_3Al_2(SiO_4)(OH)_8$ (PDF no 38-0368), Kaolinite 1 A $Al_2Si_2O_5(OH)_4$, Calcite $Ca(CO_3)$ (PDF no. 64-9630) and Cancrinite $Na_{7.6}(Al_6Si_6O_{24})(HCO_3)_{1.2}(CO_3)_{0.2}(H_2O)_{2.28}$ (PDF no. 70-5030). And iron oxide present as Hematite Fe2O3 (PDF no. 87-1164) was also detected in red mud. The amount of red mud and fly ash in the foam ceramics samples was designed to be as high as possible because the experimental purpose was the comprehensive utilization of red mud and fly ash. The sample with the amount of red mud in the range of 40–60 wt% and fly ash in the range of 20–40 wt% has been prepared and the properties have been studied in detail.

Sodium silicate, as an additive, which was introduced into a ceramic foam batch in small quantities is called a

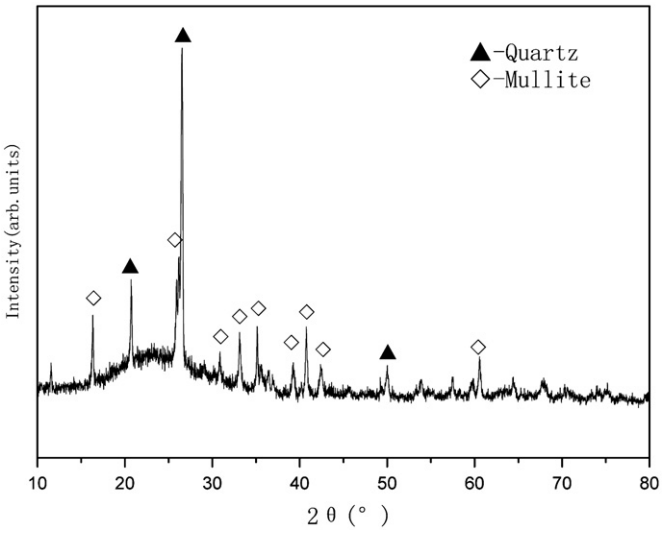

Fig. 1. XRD pattern of the fly ash.

Table 1
Chemical composition (wt%) of fly ash and red mud.

Raw materials	SiO_2	Al_2O_3	Na_2O	K_2O	MgO	CaO	Fe_2O_3	P_2O_5	MnO	TiO_2	LOI
Fly ash	54.37	24.47	1.44	1.71	0.99	4.85	5.50	0.27	0.04	1.45	4.27
Red mud	20.53	21.76	12.06	1.76	1.04	17.23	10.47	0.16	0.01	4.10	10.8

forming agent. Several processes take place under the thermal treatment of such a mixture, resulting in foam formation. Sodium borate, as an additive which could reduce the softening temperature, and was introduced into mixture is called a fluxing agent. Solid sodium borate melts at about 741 °C and reacts with R_2O ($R=Na^+$, K^+), MO ($M=Mg^{2+}$, Ca^{2+}) and partial SiO_2 in red mud and fly ash, resulting in the formation of multi-component liquid phase. On one hand, the liquid phase can accelerate the particle diffusion during sintering process, thereby reducing the sintering temperature; on the other hand, when the temperature of the mixture exceeds the softening temperature, particles start sintering and form a continuous sintered body. Particles of the pore-forming agent become insulated by softening glass. After a certain temperature is reached, they start emitting gases or losing crystal water, and frothing the glass melt. The various experimental plans are shown in Table 2.

2.2. Sample preparation

Red mud and fly ash were mixed with different amounts ranging from 20%–40% and 60%–40% of the solid weight, respectively. The compounds designed in Table 2 were combined and prepared by uniaxial dry-pressing into disk shapes with a diameter of 50 mm, thickness of 10 mm, using a pressure of 10 MPa. Then the mixtures would be used in further sintering process. The obtained green samples are firstly treated at 400 °C for 1 h in order to remove the residue water and protect the samples from cracking caused by the uneven thermal distribution. Subsequently, the samples were heated at 800–1100 °C for 2 h in an electrical furnace with air atmosphere. The heating rate of 3 °C/min was adopted during total sintering process from room temperature to 800–1100 °C.

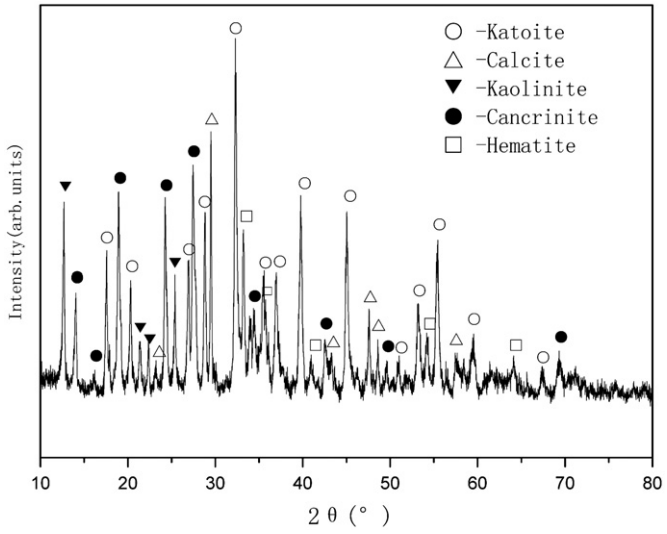

Fig. 2. XRD pattern of the red mud.

2.3. Microstructure characterization

The crystalline phases precipitated in the prepared samples are investigated by Rigaku D/max 2550PC X-ray (CuKα, scanning rate: 8°/min, scanning range: 10–80°). The surface of the sample was polished by sand paper and investigated by scanning electronic microscopy using a Quanta 200.

2.4. Porosity and water absorption

The bulk density was measured with helium psychometry. The total porosity was obtained from the bulk density and the powder density using the following equation:

$$\text{Porosity}\ (\%) = (1-\text{Bulk density}/\text{Powder density}) \times 100\% \quad (1)$$

The water absorption was measured by the waterlogged method using the following equation; we weighed the samples masses before and after saturation with water:

$$\text{Water absorption}\ (\%) = (m_2-m_1)/m_1 \times 100\% \quad (2)$$

where m_1 and m_2 are the weights of the samples before and after saturation with water.

2.5. Mechanical strength

The specimens used in the flexural strength test are machined into 20 mm × 6 mm × 7 mm test bars. Square foam

Table 2
Amount of raw materials and chemical composition provided by red mud and fly ash in different experimental plans.

Sample	Main raw material ratio (wt%)				Main chemical composition provided by red mud and fly ash (wt%)			
	Red mud	Fly ash	Sodium silicate	Sodium borate	SiO_2	Al_2O_3	Alkaline oxides	Alkaline earth oxides
A1	40	40	5	15	29.96	18.49	6.79	9.64
A2	50	30	5	15	26.58	18.22	7.86	10.89
A3	60	20	5	15	23.19	17.95	8.92	12.13
A4	46.88	28.13	5	20	24.92	17.08	7.36	10.21
A5	43.75	26.25	5	25	23.25	15.94	6.87	9.53
A6	60	20	5	15	23.19	17.95	8.92	12.13
A7	60	20	5	15	23.19	17.95	8.92	12.13
A8	60	20	5	15	23.19	17.95	8.92	12.13

glass samples of 12.5 mm length and 5 mm × 5 mm section area are subjected to uniaxial compressive loading. The flexural strength and compressive strength are measured for specimen bars with a span of 10 mm at a cross-head speed of 1 mm/min, using a CSS44100 testing machine. Each result is the average of five measurements.

3. Results and discussion

3.1. The effects of red mud and fly ash on sample properties

In the experimental results, labeled A1, A2 and A3, effects of different ratios of red mud to fly ash on sample properties were investigated, shown in Table 3. In the sample, the raw material is red mud and fly ash, and sodium silicate is added as foaming agent and sodium bauxite as fluxing agent. The red mud contents 40 wt%, 50 wt% and 60 wt% were used in A1, A2 and A3, respectively. And also, the fly ash contents 40 wt%, 30 wt% and 20 wt% were used in A1, A2 and A3, respectively.

Fig. 3 illustrates the evolution of microstructure of the samples A1, A2 and A3 heat treated at 900 °C for 2 h. As presented in A1, the matrix is filled with majority of round shaped large pores (diameter of 1.5–2.5 mm) and minority of small pores (diameter of 0.3–0.5 mm) that can easily be inferred in accordance with the results of bulk density 0.64 g/cm^3 and porosity 69.32%. In sample A2, it presents round shaped small pores (diameter of 1.0–1.5 mm) and denser microstructure, and showed higher values of bulk density (1.13 g/cm^3) and slightly low porosity 44.33%. In sample A3, many unshaped pores were distributed in the matrix. The size and the number of the pores were obviously smaller than those in A1 and A2, with values of bulk density 1.13 g/cm^3 and porosity 33.67%. Due to the inertness of red mud, the softening temperature increased obviously with the addition of red mud, which led to high viscosity unnecessary for foaming and diminished the pore sizes.

Table 3 (A1, A2 and A3) reports sample properties versus different ratios of red mud to fly ash tested. It can be observed that sample A1 showed high water absorption with value 6.02%. Sample A2 had lower water absorption value 3.26%. The lowest value of 1.55% was obtained in the sample A3. It was found that water absorption of the samples decreased linearly with the addition of red mud. Apparently, the water absorption of the porous ceramics was related to the amount of waste residue that was added. Essentially, water absorption was directly related to the porosity, and correlated with the number of open pores in sample appearance. In short, the porosity of the products increases, and the water absorption falls.

The flexural strengths of the sample A1, A2 and A3 were 2.31 MPa, 6.25 MPa and 11.25 MPa, respectively. And the corresponding compressive strengths vary from 4.04 MPa, 9.52 MPa to 17.29 MPa. Both compressive strength and flexural strength increase with the increase of red mud percentage. Moreover, higher porosity led to lower mechanical strength. As shown, it can be concluded that a negative correlation between mechanical strength and water absorption is obtained in this foam ceramics.

Fig. 4 illustrates the XRD patterns of the sample with the various proportions of red mud and fly ash. It can be seen that no Nepheline $KNa_3Al_4Si_4O_{16}$ (PDF no. 74-1718)

Table 3
Sample properties of the eight experimental plans.

Sample	A1	A2	A3	A4	A5	A6	A7	A8
Bulk density (g/cm^3)	0.64	1.13	1.63	0.60	0.51	1.52	1.19	1.67
Powder density (g/cm^3)	2.08	2.03	2.47	8.84	14.77	1.96	1.91	2.32
Porosity (%)	69.32	44.33	33.67	74.15	64.14	22.83	37.72	28.10
Water absorption (%)	6.02	3.26	1.55	2.31	4.68	2.69	1.48	1.32
Flexural strength (MPa)	2.31	6.25	11.25	8.52	4.74	6.93	8.21	5.02
Compression strength (MPa)	4.04	9.52	17.29	10.63	6.32	15.78	15.46	13.64

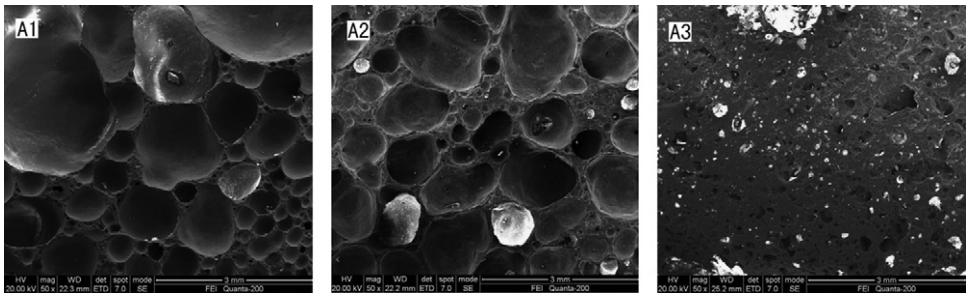

Fig. 3. SEM images of sample A1 (40 wt% red mud, 40 wt% fly ash), A2 (50 wt% red mud, 30 wt% fly ash), and A3 (60 wt% red mud, 20 wt% fly ash).

phase is observed in A1. With content of red mud increased to 50 wt% or 60 wt%, nepheline phase appears in A2 and A3. The major phases in these three samples are Hauyne $K_{1.4}Ca_{2.4}Na_{4.32}(Al_6Si_6O_{24})(SO_4)_{1.52}$ (PDF no. 78–2490) and Andradite $Ca_3Fe_2(SiO_4)_3$ (PDF no. 84-2160). By increasing the amount of red mud, the peak intensity of nepheline phase and hauyne phase increased, but the peak intensity of glass phase in these three samples gradually decreased. Mostly, the peak intensity of andradite phase in A2 is stronger than that in A1 and A3. According to these phenomena above, it can be inferred that, phase transformation exists here, including glass phase changed into nepheline phase, and andradite phase changed into hauyne phase or nepheline phase. This was seemingly achieved due to the change of the content of raw materials (red mud and fly ash) and especially the replacement among ions occurred in structure vacancy.

3.2. The effect of sodium borate on sample properties

In the experimental results, labeled A2, A4 and A5, the influences of sodium borate content on sample properties were investigated, shown in Table 2. In the sample, sodium borate contents of 15 wt%, 20 wt% and 25 wt% were used in A2, A4 and A5, respectively.

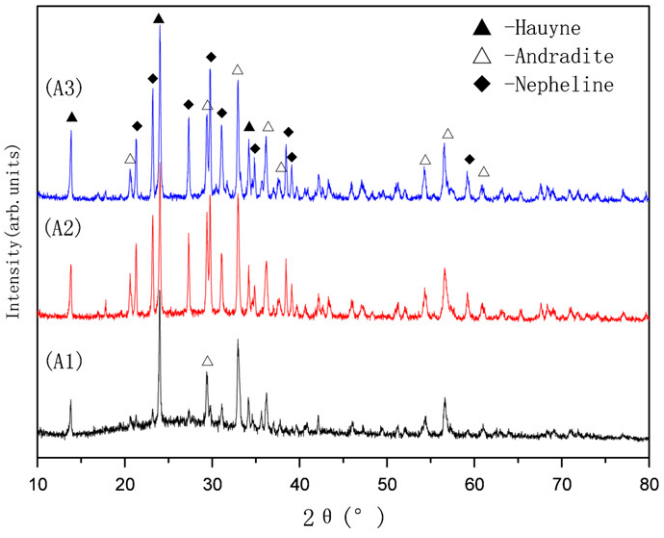

Fig. 4. XRD patterns of samples A1, A2 and A3.

Fig. 5 clearly illustrates the evolution of microstructure of samples A2, A4 and A5 heat treated at 900 °C for 2 h. The morphology of A2 has been described above. In sample A4, the round shape pores (diameter 1–1.5 mm) were formed in the matrix, with values of porosity 74.15%, and bulk density 0.60 g/cm^3. Moreover, from Fig. 5 (A4), pores were distributed uniformly in the matrix and formed homogeneous structure which contributes more to the mechanical strength. In sample A5, the pores present mainly in large scale (diameter 1.5–3 mm), irregular shape and non-uniform distribution in the matrix, with porosity 64.14%, and bulk density 0.51 g/cm^3. Pores with uniform distribution result in high porosity obtained by A4 than other samples with non-uniformly distributed pores.

Table 3 (A2, A4 and A5) reports sample properties versus different contents of sodium borate tested. It was found that water absorption decreases with sodium borate percentage at first and increases later. The water absorptions of samples A2, A4 and A5 were 3.26%, 2.31% and 4.68%, respectively. The evolution of the water absorption also fits well with the sintering behavior of ceramics affected by the formation of a "transitory liquid" phase which improves densification of the green body. Proper percentage of sodium borate is necessary for the densification of sample body and foam formation in the matrix (not on the matrix surface). The effects caused by sodium borate percentage mainly include: (i) small amount of fluxing agents, in the matrix at 900 °C, cannot sufficiently make the matrix softened in the sintering process and formed densification body adversely. Due to the pressing caused by physical block, the foam formed by foaming agents cannot grow in this unsoftened matrix, (ii) excess amounts of fluxing agent, tend to enhance the softening ability of the system. And on the surface of sample at 900 °C, high content of sodium borate caused serious collapse phenomenon. The foam formed by foaming agents can easily cross the matrix and form large open pores in the sample surface. Also, the high value of water absorption in A5 is most probably due to large open pores present in the sample surface.

The influence of sodium borate content on mechanical strength was investigated, also presented in Table 3 (A2, A4 and A5). The relationship between mechanical strength and water absorption also presents a negative correlation as we described above. As shown, the mechanical strength

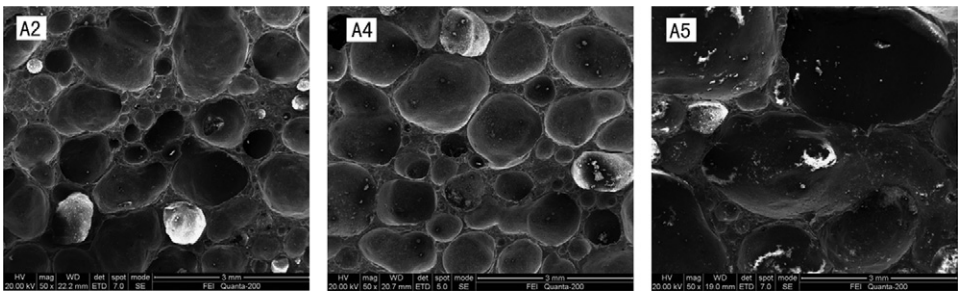

Fig. 5. SEM images of samples A2, A4 and A5 with 15 wt%, 20 wt% and 25 wt% sodium silicate content, respectively.

increases with the increase of sodium borate percentage at first and decreases later. The flexural strengths of samples A2, A4 and A5 were 6.25 MPa, 8.52 MPa and 4.74 MPa, respectively. And the corresponding compressive strengths vary from 9.52 MPa, 10.63 MPa to 6.32 MPa. Sample A4 with high porosity exhibits relatively high mechanical strength value. This phenomenon can be ascribed to porous structure (including the number, the denser microstructure, and uniform distribution of the pore) of the produced materials. While carrying out mechanical test on the samples with uniformly distributed pores, the area which can be effectively contacted with plunger tip on the surface gets larger and the force can be well distributed on the samples. So under the condition of loading force, high stress would be used to damage the samples.

Fig. 6 (A2, A4 and A5) shows the XRD patterns of the foam ceramics with sodium borate contents 15 wt%, 20 wt% and 25 wt%. The crystalline phase present in the samples corresponds to hauyne, nepheline and andradite. The peak intensity of andradite could be simply compared and described by A2 > A4 > A5. But peak intensities of hauyne and nepheline, in these three samples, show the same correlation with A4 > A2 > A5. With the amount of sodium borate increasing, it caused the transformation in crystalline phase and most probably due to the chain silicate structure of the crystalline phase it enables solubility of various ions in their structure.

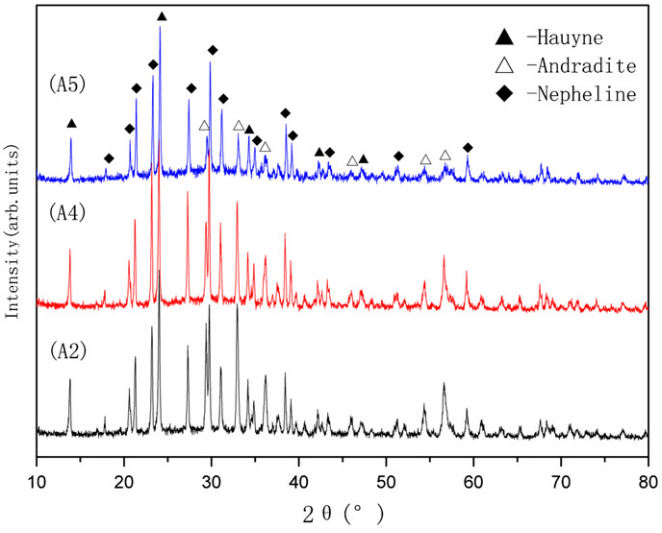

Fig. 6. XRD patterns of samples A2, A4 and A5.

Thus, calcium, magnesium, iron and aluminum might occupy structure vacancy and cause this transformation.

3.3. The effect of heat-treatment temperature on sample properties

In the experimental results, labeled A3, A6, A7 and A8, effects of sintering temperature on sample properties were investigated, shown in Table 2. In the sample, the sintering temperatures of 800 °C, 900 °C, 1000 °C and 1100 °C were used in A6, A3, A7 and A8, respectively.

Fig. 7 schematically illustrates the evolution of microstructure for the samples heat treatment at 800–1100 °C. Round shape pores with diameter of 1 mm were gradually formed at 1000°C. The samples sintered at lower temperatures (800 and 900 °C) showed a denser microstructure, and many of the unformed pores (100 μm in diameter) in A6 (with porosity 22.83%) and A3 (with porosity 33.67%) can be clearly seen from the SEM images. With sintering at higher temperature (1200 °C), the sample exhibits a characteristic of relatively quick densification which is well verified by the quick increase in bulk density (1.67 g/cm^3). And the quantity of pores (1.5 mm in diameter) in A8 (with porosity 28.10%), was obviously less than that in A7 (with porosity 37.72%). This was seemingly achieved due to a higher liquid phase viscosity.

As shown in Table 3 (A6, A3, A7 and A8), when the proportion of the raw materials was fixed as red mud 60 wt%, fly ash 20 wt%, sodium silicate 5 wt% and sodium borate 15 wt%, their properties were less sensitive to temperature variations. It was found that as the sintering temperature increases, the water absorption decreases. The result was influenced by the densification sintering degree under different sintering temperatures. The mechanical strength displayed the nonlinear trend with the heat treatment temperature increasing. As the temperature from 800 to 900 °C, the flexural strength increased from 6.93 MPa to 15.78 MPa and the compression strength increased from 15.78 MPa to 17.29 MPa. But when the temperature exceeds 900 °C, the flexural strength and compression strength decreased from 11.25 MPa to 5.02 MPa and 17.29 MPa to 13.64 MPa, respectively. Also, the measurement (such as the test method, sample preparation and calculation) caused relatively small impacts in sample properties. For the foam materials, it

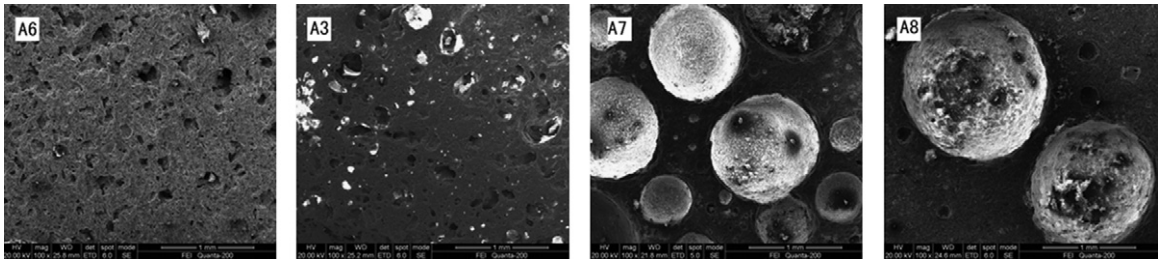

Fig. 7. SEM images of samples A6, A3, A7 and A8 sintered at 800 °C, 900 °C, 1000 °C and 1100 °C, respectively.

is very difficult to prepare the samples with the so-called regular shape. A small difference in size will lead to a major change of density, thereby affecting the calculated results of porosity according to equation.

4. Conclusions

The study highlighted the feasibility of recycling red mud in the aluminum industries and fly ash in the thermal power plant with producing foam ceramics techniques. The results presented and discussed along with this work enable to draw the following conclusions: (i) with the amount of red mud increasing, the sample shows poor sintering activity. This phenomenon can be ascribed to the complicated and refractory crystalline phase contained in red mud and this caused the inertness of red mud. The softening temperature of the mixture raised and that led to the sample, which contains high amount of red mud, hardly softening. Therefore, the pore formed by sodium silicate could not growth sufficiently under the compact and unsoftened sintered body, (ii) the sodium borate could effectively decrease the softening temperature of the mixture; when adding just 20 wt% sodium borate, the sample presents relatively high porosity 74.15% and low bulk density 0.60 g/cm^3, (iii) the sample properties were less sensitive to different sintering temperature (800, 900, 1000, and 1100 °C for 2 h) variations, (iv) uniform distribution of pores can enhance the porosity, mechanical strength, and lower water absorption.

In this study, authors prepared foam ceramics using red mud and fly ash as raw materials simultaneously. The total amount of both the industrial solid wastes of fly ash and red mud is up to 80 wt%, which promises less raw materials cost, prominent economic benefits and environmental benefits. The foam ceramics show good performance of thermal and sound insulation, due to the high porosity, thus they are energy saving materials. Moreover, the foam ceramics may have a good application in the market of the light, the non-load bearing structure material outside the building wall system, and may play an important role to eliminate the storage of fly ash and red mud in China.

Acknowledgments

This work has been supported by the Key Project Foundation of Science and Technology Plans of Changsha in China (no.K1003027-11). The authors also gratefully acknowledge the Henan Aluminum Co. Ltd. and the Changsha Power Plant for providing the raw materials.

References

[1] A. Xenidis, A.D. Harokopou, E. Mylona, G. Brofas, Modifying alumina red mud to support a revegetation cover, JOM—Journal of Minerals Metals and Materials Society 57 (2005) 42–46.
[2] A. Bhatnagar, V.J.P. Vilar, C.M.S. Botelho, R.A.R. Boaventura, A review of the use of red mud as adsorbent for the removal of toxic pollutants from water and wastewater, Environmental Technology 32 (2011) 231–249.
[3] C. Brunori, C. Cremisini, P. Massanisso, V. Pinto, L. Torricelli, Reuse of a treated red mud bauxite waste: studies on environmental compatibility, Journal of Hazardous Materials 117 (2005) 55–63.
[4] Z.H. Pan, L. Cheng, Y.N. Lu, N.R. Yang, Hydration products of alkali-activated slag-red mud cementitious material, Cement and Concrete Research 32 (2002) 357–362.
[5] M. Ahmaruzzaman, A review on the utilization of fly ash, Progress in Energy and Combustion Science 36 (2010) 327–363.
[6] C.L. Carlson, D.C. Adriano, Environmental impacts of coal combustion residues, Journal of Environmental Quality 22 (1993) 227–247.
[7] K.C. Vasilopoulos, D.U. Tulyaganov, S. Agathopoulos, M.A. Karakassides, J.M.F. Ferreira, D. Tsipas, Bulk nucleated fine grained mono-mineral glass-ceramics from low-silica fly ash, Ceramics International 35 (2009) 555–558.
[8] Y. Li, C. Liu, Z. Luan, X. Peng, C. Zhu, Z. Chen, Z. Zhang, J. Fan, Z. Jia, Phosphate removal from aqueous solutions using raw and activated red mud and fly ash, Journal of Hazardous Materials 137 (2006) 374–383.
[9] B. Karasu, E. Agun, G. Kaya, Effects of red mud based pigments on wall and floor tile glazes, CFI—Ceramic Forum International (2005) E41–E44.
[10] S.S. Amritphale, A. Anshul, N. Chandra, N. Ramakrishnan, A novel process for making radiopaque materials using bauxite—red mud, Journal of the European Ceramic Society 27 (2007) 1945–1951.
[11] S.D. Yoon, Y.H. Yun, An advanced technique for recycling fly ash and waste glass, Journal of Materials Processing Technology 168 (2005) 56–61.
[12] C. Leroy, M. Ferro, R. Monteiro, M. Fernandes, Production of glass-ceramics from coal ashes, Journal of the European Ceramic Society 21 (2001) 195–202.
[13] H. Yang, C. Chen, L. Pan, H. Lu, H. Sun, X. Hu, Preparation of double-layer glass-ceramic/ceramic tile from bauxite tailings and red mud, Journal of the European Ceramic Society 29 (2009) 1887–1894.
[14] V.M. Sglavo, S. Maurina, A. Conci, A. Salviati, G. Carturan, G. Cocco, Bauxite 'red mud' in the ceramic industry. Part 2. Production of clay-based ceramics, Journal of the European Ceramic Society 20 (2000) 245–252.
[15] J. Yang, D. Zhang, J. Hou, B. He, B. Xiao, Preparation of glass-ceramics from red mud in the aluminium industries, Ceramics International 34 (2008) 125–130.
[16] C. Dry, J. Meier, J. Bukowski, Sintered coal ash/flux materials for building materials, Materials and Structures 37 (2004) 114–121.
[17] Z.R. Niu, Y.H. Jiang, Y.Y. Luo, Study on engineering characteristics of foamed glass system of heat preservation and thermal insulation of building wall, in: Proceedings of the advances in Heterogeneous Material Mechanics 2008–2nd International Conference on Heterogeneous Material Mechanics, ICHMM 2008, June 3, 2008–June 8, 2008, DEStech Publications Inc., Huangshan, China, 2008, pp. 905–908.
[18] B. Chen, Z. Luo, A. Lu, Preparation of sintered foam glass with high fly ash content, Materials Letters 65 (2011) 3555–3558.
[19] B. Chen, K. Wang, X. Chen, A. Lu, Study of foam glass with high content of fly ash using calcium carbonate as foaming agent, Materials Letters 79 (2012) 263–265.